

UC San Diego

UC San Diego Previously Published Works

Title

Restriction spectrum imaging of white matter and its relation to neurological disability in multiple sclerosis

Permalink

<https://escholarship.org/uc/item/0gk3c6fp>

Journal

Multiple Sclerosis Journal, 25(5)

ISSN

1352-4585

Authors

Sowa, Piotr
Harbo, Hanne F
White, Nathan S
[et al.](#)

Publication Date

2019-04-01

DOI

10.1177/1352458518765671

Peer reviewed

Restriction spectrum imaging of white matter and its relation to neurological disability in multiple sclerosis

Piotr Sowa, Hanne F Harbo, Nathan S White, Elisabeth G Celius, Hauke Bartsch, Pål Berg-Hansen, Stine M Moen, Atle Bjørnerud, Lars T Westlye, Ole A Andreassen, Anders M Dale  and Mona K Beyer

Abstract

Background: Restriction spectrum imaging (RSI) is a recently introduced magnetic resonance imaging diffusion technique. The utility of RSI in multiple sclerosis (MS) is unknown.

Objective: To investigate the association between RSI-derived parameters and neurological disability in MS.

Methods: Seventy-seven relapsing–remitting MS patients were scanned with RSI on a 3-T scanner. RSI-derived parameters: fast and slow apparent diffusion coefficient (sADC), fractional anisotropy, restricted fractional anisotropy, neurite density (ND), cellularity, extracellular water fraction, and free water fraction, were obtained in white matter lesions (WML) and normal appearing white matter (NAWM). Patients were divided into three groups according to their expanded disability status scale (EDSS): with minimal, low, and substantial disability (<2.5, 2.5–3, and >3, respectively). Group comparisons and correlation analyses were performed.

Results: All tested RSI-derived parameters differed between WML and NAWM ($p < 0.001$ for all pairwise comparisons). The sADC in WML showed largest difference across disability subgroups (analysis of variance (ANOVA): $F = 5.1$, $\eta^2 = 0.12$, $p = 0.008$). ND in NAWM showed strongest correlation with disability ($\rho = -0.39$, $p < 0.001$).

Conclusion: The strongest correlation with EDSS of ND obtained in NAWM indicates that processes outside lesions are important for disability in MS. Our study suggests that RSI-derived parameters may help understand the “clinico-radiological paradox” and improve disease monitoring in MS.

Keywords: Magnetic resonance imaging, multiple sclerosis, restriction spectrum imaging, neurite density, neurological disability

Date received: 13 September 2017; revised: 7 February 2018; accepted: 23 February 2018

Introduction

Multiple sclerosis (MS) is a chronic inflammatory disease of the central nervous system primarily affecting young adults and often resulting in severe neurological disability.¹ Even though magnetic resonance imaging (MRI) has become an important tool in the diagnostics and follow-up of MS patients,^{2,3} there is a need for new imaging markers to improve the diagnostic and therapeutic precision.² Diffusion MRI is a promising technique in MS. The technique is based on measuring the random Brownian motions of water molecules within tissue. Standard diffusion-weighted imaging (DWI) provides the apparent diffusion

coefficient (ADC), a measure that helps in early detection of ischemic regions in stroke and can differentiate between various pathological conditions.⁴ More advanced techniques have enabled calculation of ADC for the fast and slow diffusion components: fast apparent diffusion coefficient (fADC) and slow apparent diffusion coefficient (sADC), in theory corresponding to the extracellular and intracellular water compartments.⁵ Diffusion tensor imaging (DTI) is a multidirectional diffusion MRI⁶ that provides fractional anisotropy (FA) which is a scalar value between 0 and 1, where value of 0 means equal diffusion in all

Multiple Sclerosis Journal

1–12

DOI: 10.1177/
1352458518765671

© The Author(s), 2018.
Reprints and permissions:
[http://www.sagepub.co.uk/
journalsPermissions.nav](http://www.sagepub.co.uk/journalsPermissions.nav)

Correspondence to:

P Sowa
Division of Radiology
& Nuclear Medicine,
Oslo University Hospital,
Kirkeveien 166, P.O. Box
4956, Nydalen, 0424 Oslo,
Norway.

piotr.sowa@medisin.uio.no

Piotr Sowa
Division of Radiology &
Nuclear Medicine, Oslo
University Hospital, Oslo,
Norway/Institute of Clinical
Medicine, University of Oslo,
Oslo, Norway

Hanne F Harbo
Pål Berg-Hansen
Institute of Clinical
Medicine, University
of Oslo, Oslo, Norway/
Department of Neurology,
Oslo University Hospital,
Oslo, Norway

Stine M Moen
Department of Neurology,
Oslo University Hospital,
Oslo, Norway/MS Centre
Hakadal, Hakadal, Norway

Nathan S White
Hauke Bartsch
Department of Radiology,
University of California, San
Diego, La Jolla, CA, USA

Elisabeth G Celius
Department of Neurology,
Oslo University Hospital,
Oslo, Norway/Institute
of Health and Society,
University of Oslo, Oslo,
Norway

Atle Bjørnerud
Division of Radiology &
Nuclear Medicine, Oslo
University Hospital, Oslo,
Norway/Department of
Physics, University of Oslo,
Oslo, Norway

Lars T Westlye
Department of Psychology,
University of Oslo, Oslo,
Norway/NORMENT K.G.
Jebsen Centre for Psychosis
Research, Oslo University
Hospital, Oslo, Norway

Ole A Andreassen
NORMENT K.G. Jebsen

Centre for Psychosis
Research, Oslo University
Hospital, Oslo, Norway

Anders M Dale

Department of Radiology,
University of California,
San Diego, La Jolla,
CA, USA/Department of
Neurosciences, University
of California, San Diego, La
Jolla, CA, USA

Mona K Beyer

Division of Radiology &
Nuclear Medicine, Oslo
University Hospital, Oslo,
Norway/Department of Life
Sciences and Health, Oslo
and Akershus University
College of Applied Sciences,
Oslo, Norway

directions and value of 1 means diffusion restricted to one direction only.

In MS, the diffusion MRI has been used to investigate differences between various types of lesions⁷ or lesions and normal appearing white matter (NAWM),⁸ between MS patients and healthy controls,^{9,10} as well as to study diffusion parameters in relation to clinical measures.^{10–12} However, the results of DWI and DTI studies in relation to neurological disability in MS are not consistent. Temel et al.¹¹ reported no correlation between FA and ADC in lesions or NAWM and neurological disability as measured by the expanded disability status scale (EDSS),¹³ which was in line with a previous report from 2006 by Phuttharak et al.¹⁴ Yet Gratsias et al.¹⁰ and Anik et al.¹⁵ reported a significant correlation between ADC in NAWM and EDSS scores in MS patients. The inconsistent findings can be partly explained by different methodologies and different definitions of NAWM across the studies.

The non-specific nature of ADC and known limitations of DTI in describing diffusion in nonhomogeneous media¹⁶ have stimulated development of more advanced diffusion techniques like high-angular resolution diffusion imaging (HARDI) and neurite orientation dispersion and density imaging (NODDI).¹⁷ Restriction spectrum imaging (RSI) is a recently introduced MRI technique that is based on measuring water diffusion probed with multiple *b*-values and various directions. RSI is a straightforward extension of HARDI;¹⁸ it enables more specific estimation of tissue microstructure compared to DWI and DTI¹⁹ and has shown promising results in neuroradiology attempting to improve tumor delineation,²⁰ recover white matter (WM) tracts in peritumoral regions²¹ and better reflect WM pathology in temporal lobe epilepsy²² as well as in oncologic imaging.¹⁹ In addition to the above-mentioned DWI and DTI diffusion parameters, RSI also enables calculation of restricted fractional anisotropy (rFA), neurite density (ND), cellularity, extracellular water fraction (EWF), and free water fraction (FWF), described in more details below. These parameters provide additional information on brain tissue that may be of clinical importance in MS.

The utility of RSI in MS has not been investigated. The purpose of this study was to explore the RSI-derived diffusion parameters in white matter lesions (WML) and NAWM, and to evaluate their association with neurological disability in MS.

Materials and methods

Participants

Seventy-seven relapsing–remitting (RR) MS patients, diagnosed according to the current diagnostic criteria,²³ were included. The patients were recruited and referred to MRI by treating neurologists at our institution in the period 2013–2014. Mean age of the patients was 39.9±10.3 years (range 20–67), whereof 60 females (mean age 39.1±10.4 years, range 20–64) and 17 males (mean age 42.6±9.9 years, range 27–67). The patients were included at different clinical stages (described in detail in the Results paragraph). The inclusion criteria were patient age of more than 18 years, no prior neurological disease, no contraindication for MRI, and no allergy to gadolinium-based contrast media. Since the study was performed in an ambulatory setting, we excluded patients completely restricted to bed or wheelchair and unable to move themselves onto the scanner table. Of 94 patients that met the inclusion criteria and were scanned with the RSI sequence, 17 were excluded, mainly due to technical reasons related to image postprocessing. The flowchart for patient inclusion is shown in Supplementary material 1.

Clinical data

The following clinical and laboratory data were collected from the patients' electronic hospital record: age at disease onset, disease duration, disease subtype, neurological disability assessed with EDSS, and type of disease modifying treatment (shown in Supplementary material 2). EDSS from the date closest to the MRI acquisition was collected and multiple sclerosis severity score (MSSS)²⁴ was determined. Details concerning demographical, clinical, and laboratory data of the patient cohort are shown in Table 1.

Clinical subgroups

The patients were divided into clinical subgroups based on their neurological disability as measured by EDSS score: group 1 (*n*=28) had minimal disability and EDSS of <2.5; group 2 (*n*=41) had low disability and EDSS of 2.5–3; and group 3 (*n*=11) had moderate to substantial disability and EDSS of >3 (hereafter referred to as “substantial disability”). Since the patients in general had relatively low disability as reflected in a median EDSS of 2.0 (interquartile range 1–2.75, range 0–6.5), we used an EDSS threshold of 2.0 and 3.0 to divide the patients into three groups with different disability levels in the analysis. The choice of cut-off of 3.0 resulted in a larger group with higher disability (*n*=11).

Table 1. Demographic and clinical characteristics^a, *n* = 77.

Age, years	39.9 ± 10.3, range 20–67
Females	60 (78%)
Age at disease onset, years	27 (25–35), range 16–53
Disease duration, years	9 (4–13.5), range 1–32
Relapsing–remitting phenotype	77 (100%)
EDSS	2.0 (1–2.75), range 0–6.5
MSSS	2.34 (0.99–4.25), range 0.05–8.91
Disease modifying treatment ^b (patients <i>n</i> =)	
No treatment	24 (31%)
First line	22 (29%)
Second line	30 (39%)
Third line	1 (1%)
Oligoclonal bands in CSF (patients <i>n</i> =)	
Yes	70 (91%)
No	6 (8%)
Unknown	1 (1%)

CSF: cerebrospinal fluid; EDSS: expanded disability status scale; MSSS: multiple sclerosis severity score.
^aData are *n* (%) for nominal variables, mean ± standard deviation for normally distributed variables, or median (interquartile range) for non-normally distributed variables.
^bDisease modifying treatment is explained in details in Supplementary material 2.

Image acquisition

The RSI sequence used in our study was available through an inter-institutional collaboration. All MRI scans were acquired on a 3-T scanner (Signa Optima HDxt, General Electric, Fairfield, CT, USA). Sixty-nine patients were scanned using an 8-channel head coil and eight patients using a 12-channel head coil, due to different availability of these coils to us during the period of data collection at our site. The distribution of clinical parameters (age, age at disease onset, disease duration, EDSS, and MSSS) was not significantly different between the two groups and all patients were included in the final analysis. The imaging protocol included the following sequences:

1. Sagittal 3D T1-weighted fast spoiled gradient echo (FSPGR) (time of echo (TE) = 3–12 ms; time of repetition (TR) = 7.8 ms; time of inversion (TI) = 450 ms; FA = 12°; field of view (FOV) = 25.6 cm; matrix = 256 × 192 mm; slice thickness = 1.2 mm);
2. Sagittal 3D T2-weighted FLAIR CUBE (TE/TR = 126.5/6000 ms; TI = 1861 ms; FOV = 25.6 cm, matrix = 256 × 256 mm, slice thickness = 1 mm);
3. Axial single-shot spin-echo diffusion-weighted echo-planar multishell RSI sequence (TE = 96–289 ms; TR = 17 s; FA = 90°; FOV = 24 cm; matrix = 96 × 96 mm; slice thickness = 2.5 mm, acquired with *b* = 0, 500, 1500, and 4000 s/mm² with 6, 6, and 15 unique gradient directions for

each nonzero *b*-value, respectively); Figure 1 shows RSI sequence as raw images acquired with the different *b*-values in a sample patient;

4. Post-gadolinium sagittal 3D T1-weighted sequence, with parameters identical to those of pre-gadolinium 3D T1, acquired approximately 5 minutes after intravenous contrast agent injection at a dose of 0.2 mL/kg (Dotarem, Laboratoire Guerbet, Paris, France).

Image analysis

1. The preprocessing, RSI processing, and co-registration of image data were performed using in-house software developed in MATLAB (MathWorks, Natick, MA, USA). The RSI diffusion data were corrected offline for spatial distortions, postprocessed in native space and then the derived RSI images were resampled and co-registered to the structural series (also corrected for distortions and registered to each other). The image data from each participant were visually inspected for quality control. FA was calculated from all *b*-values: *b* = 0, 500, 1500, and 4000 s/mm², fADC was calculated from *b* = 500 data and sADC from the *b* = 4000 data (the RSI-derived fADC and sADC are not equal to DTI-derived ADC, which is usually calculated from an intermediate *b*-value). The rFA was calculated from a tensor fit to the restricted water signal derived from the RSI

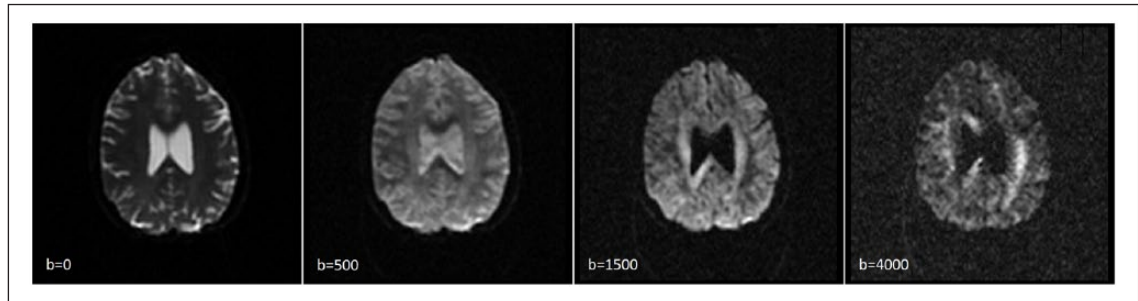


Figure 1. RSI sequence shown as raw images with different b -values in a patient. From the left: images acquired with b -values of 0, 500, 1500, and 4000 s/mm^2 with 6, 6, and 15 unique gradient directions for each nonzero b -value, respectively. The raw RSI data were used to obtain the RSI parameter maps. RSI: restriction spectrum imaging.

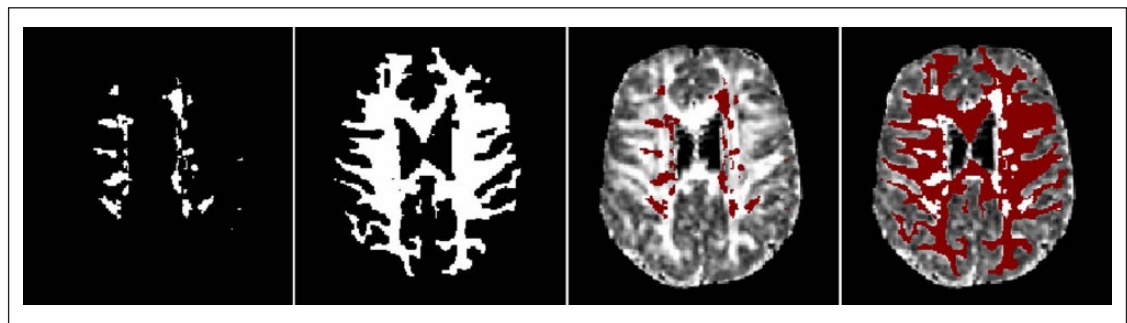


Figure 2. Co-registered binary masks and rFA map in a sample patient. Here we see from the left: WML mask, WM mask, a sample map (here shown rFA map) with overlaid WML mask (brown), and the same rFA map with overlaid WML and WM masks showing NAWM region (brown). Values of the RSI-derived parameters were obtained from the whole volume of WML and the whole volume of NAWM. NAWM: normal appearing white matter; rFA: restricted fractional anisotropy; WM: white matter; WML: white matter lesions.

model, with optimal sensitivity to cylindrically restricted diffusion. Also ND, cellularity, EWF, and FWF were calculated. RSI processing is described in details in a method paper with theoretical and histological validation of the RSI sequence.¹⁸

2. Semi-automated WML segmentation was performed by two radiologists in all 77 subjects using in-house software and MIPAV software (v.7.2.0, Center for Information Technology, National Institutes of Health, Bethesda, MD, USA). The first author performed final visual inspection of the WML masks in each patient using MIPAV software. The 3D FLAIR series was used for the WML segmentation. As a result, a WML mask representing all lesions was created for each patient.
3. FreeSurfer software (www.freesurfer.net) was used to segment the 3D T1 series to create masks of WM and grey matter (GM), and to obtain volumetric parameters. The masks were visually inspected and corrected for segmentation

errors using the same software. WM volume was calculated using a “lesion filling” approach in nordicICE software (www.nordicneurolab.com)—first the NAWM volume was calculated (using WM mask as inclusion mask and WML mask as exclusion mask) and then the volumes of NAWM and WML were summarized. Nordic Ice was chosen for this purpose because the software was available and well known to us and it was previously used for imaging post-processing in MS.^{25,26}

4. The diffusion parameters were extracted from the whole volume of WML and from the NAWM. For each patient, we calculated fADC, sADC, FA, rFA, ND, cellularity, EWF, and FWF mean values in WML and in NAWM. Figure 2 shows schematically WML and WM masks, and the rFA map with and without mask overlays in a sample patient. The parameters are described in detail in Supplementary material 3. The fADC is more sensitive to changes in extracellular diffusion compared

with sADC, but they should not be simply ascribed to specific microcompartments as they are not based on the RSI model. The rFA is the FA derived from the restricted signal from cylindrical structures. ND is the signal fraction of cylindrically restricted water, reflecting the density of neurites in tissue. The EWF represents the signal fraction of water that is hindered due to tortuous geometry of the extracellular space while the FWF is the signal fraction of freely diffusing water.

Statistical analyses

Statistical analyses were performed with the Statistical Package for the Social Sciences software (SPSS v24, IBM, Chicago, IL, USA). In addition, the “R” statistical software (v3.1.1, www.r-project.org) was used for the Benjamini–Hochberg false discovery rate method to control for multiple tests. For group comparisons between two groups, the parametric independent samples *t*-test was used when the data were normally distributed; otherwise, the non-parametric Mann–Whitney *U* test was used. For group comparisons between three or more groups, the parametric one-way analysis of variance (ANOVA) test was used (corrected for multiple comparisons with post-hoc Bonferroni test) when the data were normally distributed; otherwise, the non-parametric Kruskal–Wallis *H* test was used (with post-hoc Mann–Whitney *U* test and Bonferroni correction for multiple comparisons). The non-parametric Wilcoxon signed-rank test was used to test differences in diffusion parameters between WML and NAWM. Spearman’s ρ (rho) was used for assessing correlations between clinical measures and diffusion parameters as the data were non-normally distributed; otherwise, Pearson’s *r* was used for assessing partial correlations (controlled for age). All reported *p*-values are two-sided and $p < 0.05$ was defined as level of significance.

Ethical approvals

Approval for this study was obtained from the data inspectorate representative at the hospital and from the Regional Committee for Medical and Health Research Ethics. A signed informed consent was obtained from all study participants.

Results

Clinical characteristics

Demographic and clinical characteristics are shown in details in Table 1. The median age of disease onset

was 27 years (range 16–53), median disease duration at inclusion in the study was 9 years (range 1–32), and the median EDSS score was 2.0 (range 0–6.5). Median difference between EDSS date and MRI acquisition date was 2 months (range 0–8). Fifty-three patients (69%) were receiving disease modifying treatment.

Radiological findings

Detailed radiological characteristics are shown in Table 2. Confluent lesions were present in 42 patients (54%). In 13 patients (17%), contrast enhancing lesions were observed; most frequently, there were one or two enhancing lesions per patient, and more than two enhancing lesions were observed in one patient only. Because of the low number of enhancing lesions, no separate analysis of these lesions was performed. The median WML volume was 5.2 mL (range 0.15–88.2).

Diffusion parameters in WML and NAWM

All the tested RSI-derived diffusion parameters differed significantly between WML and NAWM ($p < 0.001$ for all pairwise comparisons). The fADC, sADC, rFA, and FWF were higher in WML than in NAWM, while FA, ND, cellularity, and EWF were lower in WML than in NAWM (Table 2).

Comparison of subgroups defined according to disability measured by EDSS

The clinical and MRI characteristics of each disability subgroup are presented in Table 3 and the differences in RSI-derived diffusion parameters between the subgroups are shown schematically in Figure 3. The diffusion parameter that showed largest difference across disability subgroups was sADC in WML (ANOVA: $F = 5.1$, $\eta^2 = 0.12$, $p = 0.008$). Briefly, the fADC, sADC, ND, and FWF differed significantly between the disability subgroups when obtained both in WML ($p = 0.012$, $p = 0.008$, $p = 0.024$, and $p = 0.036$, respectively) and in NAWM ($p = 0.022$, $p = 0.036$, $p = 0.009$, and $p = 0.020$, respectively). Cellularity differed between the disability subgroups only when obtained in WML ($p = 0.017$) while FA and rFA differed between the subgroups only when obtained in NAWM ($p = 0.017$ and $p = 0.019$, respectively). EWF did not differ between the subgroups neither when obtained in WML nor in NAWM. Post-hoc comparisons showed the greatest differences between the subgroups with substantial disability and minimal disability. In WML, patients with substantial disability had higher fADC ($p = 0.010$), sADC ($p = 0.007$), and FWF ($p = 0.024$), and lower ND ($p = 0.019$)

Table 2. Global imaging characteristics^a, $n = 77$.

General characteristics by WML		
Distribution of WML (patients $n =$)		
Periventricular		75 (97%)
Juxtacortical		76 (99%)
Other supratentorial subcortical		75 (97%)
Infratentorial		39 (51%)
Confluent WML (patients $n =$)		
No confluent lesions		35 (46%)
Beginning confluence		14 (18%)
Definite confluent lesions		28 (36%)
Patients with enhancing WML		13 (17%)
Volumetric data		
IV, mL		1510 ± 146
Brain volume, % of IV		72 ± 4.4
White matter volume, % of IV		31 ± 2.6
Grey matter volume, % of IV		41 ± 2.6
Cortical volume, % of IV		31 ± 2.1
WML volume, mL ^b		5.2 (2–17.8), range 0.15–88.2
RSI-derived diffusion parameters ^c		
	in WML	in NAWM
fADC	1.19 ± 0.14	0.92 (0.90–0.95)
sADC	0.57 ± 0.06	0.47 (0.46–0.48)
FA	0.32 ± 0.04	0.35 (0.33–0.36)
rFA	0.70 ± 0.05	0.65 (0.62–0.66)
ND	355 ± 52	440 (423–449)
Cellularity	106 (88–144)	193 (181–206)
EFW	695 ± 28	729 (718–735)
FWF	563 ± 59	415 (406–431)
fADC: fast apparent diffusion coefficient; EWF: extracellular water fraction; FA: fractional anisotropy; FWF: free water fraction; IV: intracranial volume; NAWM: normal appearing white matter; ND: neurite density; RSI: restriction spectrum imaging; sADC: slow apparent diffusion coefficient; rFA: restricted fractional anisotropy; WML: white matter lesions.		
^a Data are n (%) for nominal variables, mean ± standard deviation for normally distributed variables, or median (interquartile range) for non-normally distributed variables.		
^b WML volume (lesion load) based on semi-automated segmentation on FLAIR series.		
^c All tested RSI-derived diffusion parameters differed significantly between WML and NAWM (Wilcoxon signed-rank test, $p < 0.001$ for all paired comparisons). Units for the parameters are given in Supplementary material 3.		

and cellularity ($p = 0.015$). In NAWM, patients with substantial disability had *higher* fADC ($p = 0.024$), sADC ($p = 0.027$), and FWF ($p = 0.024$), and *lower* FA ($p = 0.018$), rFA ($p = 0.024$), and ND ($p = 0.0125$) than patients with minimal disability. Since we used two different types of head coil, additional analyses were performed after exclusion of the relatively low number of patients scanned with the 12-channel coil ($n = 8$). Performing analyses on the remaining 69 subjects, it was still the sADC parameter in WML that discriminated best between the disability subgroups. The results of these analyses are shown with more details in Supplementary material 4.

Correlations between clinical data, and volumetric and diffusion parameters

Details concerning correlations between the clinical data and volumetric and diffusion parameters are shown in Table 4 (the p -values presented were adjusted to control for multiple tests). ND in NAWM showed strongest correlation with EDSS ($\rho = -0.39$, $p < 0.001$) of all the investigated RSI-derived diffusion parameters. Otherwise, EDSS correlated with brain volume ($r = -0.30$, $p = 0.017$) and WM volume ($r = -0.32$, $p = 0.013$) normalized to intracranial volume, and with WML volume ($r = 0.25$, $p = 0.048$)

Table 3. Comparison of subgroups defined according to disability by EDSS^a, *n* = 77..

	Neurological disability by EDSS			<i>F</i> , η^2 or <i>H</i> , w^2	<i>p</i> -value
	Minimal (EDSS of <2.5)	Low (EDSS of 2.5–3)	Substantial (EDSS of >3)		
	<i>n</i> = 27	<i>n</i> = 39	<i>n</i> = 11		
Characteristics					
Age, years	36.6 ± 8.0	41.0 ± 11.4	43.8 ± 10.2	2.5, 0.06 ^b	0.089 ^b
Age at disease onset, years	27 (25–30)	29 (26–36)	25 (22–35)	3.8, 0.05 ^c	0.147 ^c
Disease duration, years	7.0 (4–12)	9 (3–15.5)	13 (9–27)	7.0, 0.09 ^c	0.030^c
WML volume, mL	2.7 (1.2–14.1)	4.5 (2.0–16)	19.7 (9.5–31.5)	9.9, 0.13 ^c	0.007^c
Brain volume ^d , %	73.4 ± 5.6	71.8 ± 3.1	68.7 ± 3.4	4.7, 0.13 ^b	0.011^b
Diffusion parameters in WML					
fADC	1.15 ± 0.15	1.19 ± 0.13	1.30 ± 0.11	4.7, 0.11 ^b	0.012^{b,e}
sADC	0.56 ± 0.06	0.57 ± 0.05	0.62 ± 0.05	5.1, 0.12 ^b	0.008^{b,f}
FA	0.33 ± 0.05	0.32 ± 0.04	0.30 ± 0.04	2.4, 0.06 ^b	0.100 ^b
rFA	0.70 ± 0.05	0.69 ± 0.05	0.70 ± 0.04	0.1, 0.01 ^b	0.881 ^b
ND	369 ± 56	358 ± 46	319 ± 46	3.9, 0.10 ^b	0.024^{b,g}
Cellularity	120 (96–120)	108 (91–145)	88 (74–102)	8.2, 0.11 ^c	0.017^{c,h}
EWf	700 ± 27	696 ± 28	677 ± 27	2.9, 0.07 ^b	0.061 ^b
FWf	547 ± 62	563 ± 55	601 ± 52	3.5, 0.08 ^b	0.036^{b,i}
Diffusion parameters in NAWM					
fADC	0.91 (0.89–0.95)	0.92 (0.90–0.95)	0.95 (0.94–0.98)	7.7, 0.10 ^c	0.022^{c,j}
sADC	0.47 (0.46–0.47)	0.47 (0.46–0.48)	0.48 (0.47–0.50)	6.6, 0.08 ^c	0.036^{c,k}
FA	0.35 (0.33–0.36)	0.35 (0.33–0.36)	0.31 (0.29–0.35)	8.1, 0.10 ^c	0.017^{c,l}
rFA	0.65 (0.63–0.66)	0.65 (0.63–0.66)	0.61 (0.58–0.65)	7.9, 0.10 ^c	0.019^{c,m}
ND	445 (430–454)	440 (429–448)	421 (393–436)	9.4, 0.12 ^c	0.009^{c,n}
Cellularity	195 (190–207)	194 (180–207)	182 (162–193)	4.7, 0.06 ^c	0.094 ^c
EWf	729 (718–734)	728 (714–736)	729 (726–735)	0.3, <0.01 ^c	0.844 ^c
FWf	411 (398–422)	413 (406–425)	428 (415–453)	7.8, 0.10 ^c	0.020^{c,o}

EDSS: expanded disability status scale; EWf: extracellular water fraction; FA: fractional anisotropy; fADC: fast apparent diffusion coefficient; FWf: free water fraction; ND: neurite density; sADC: slow apparent diffusion coefficient; rFA: restricted fractional anisotropy; WML: white matter lesions; NAWM: normal appearing white matter; ANOVA: analysis of variance.

The *p*-values shown are corrected for multiple comparisons with post-hoc Bonferroni test (one-way ANOVA) or with post-hoc Mann–Whitney *U* test and Bonferroni correction (Kruskal–Wallis *H* test) as appropriate; *p*-values <0.05 are indicated with bold.

^aData are mean ± standard deviation for normally distributed variables, or median (interquartile range) for non-normally distributed variables.

^bOne-way ANOVA test (normally distributed data), the next to last column shows *F* and η^2 .

^cKruskal–Wallis *H* test (non-normally distributed data), the next to last column shows *H* and w^2 .

^dNormalized brain volume (in percent of intracranial volume).

^eSignificant difference between group 3 and groups 1 and 2 (*p* = 0.010 and *p* = 0.047, respectively).

^fSignificant difference between group 3 and groups 1 and 2 (*p* = 0.007 and *p* = 0.022, respectively).

^gSignificant difference between group 3 and group 1 (*p* = 0.019).

^hSignificant difference between group 3 and groups 1 and 2 (*p* = 0.015 and *p* = 0.039, respectively).

ⁱSignificant difference between group 3 and group 1 (*p* = 0.031).

^jSignificant difference between group 3 and group 1 (*p* = 0.024).

^kSignificant difference between group 3 and group 1 (*p* = 0.027).

^lSignificant difference between group 3 and group 1 (*p* = 0.018).

^mSignificant difference between group 3 and groups 1 and 2 (*p* = 0.024 and *p* = 0.033, respectively).

ⁿSignificant difference between group 3 and groups 1 and 2 (*p* = 0.012 and *p* = 0.039, respectively).

^oSignificant difference between group 3 and groups 1 and 2 (*p* = 0.042 and *p* = 0.048, respectively).

normalized to WM volume (correlations controlled for age). For correlations with disease duration, see Table 4. MSSS did not correlate with any of the investigated diffusion or volumetric parameters.

Discussion

In the current study, we found that sADC in WML showed largest difference across EDSS subgroups, while ND in NAWM showed strongest correlation

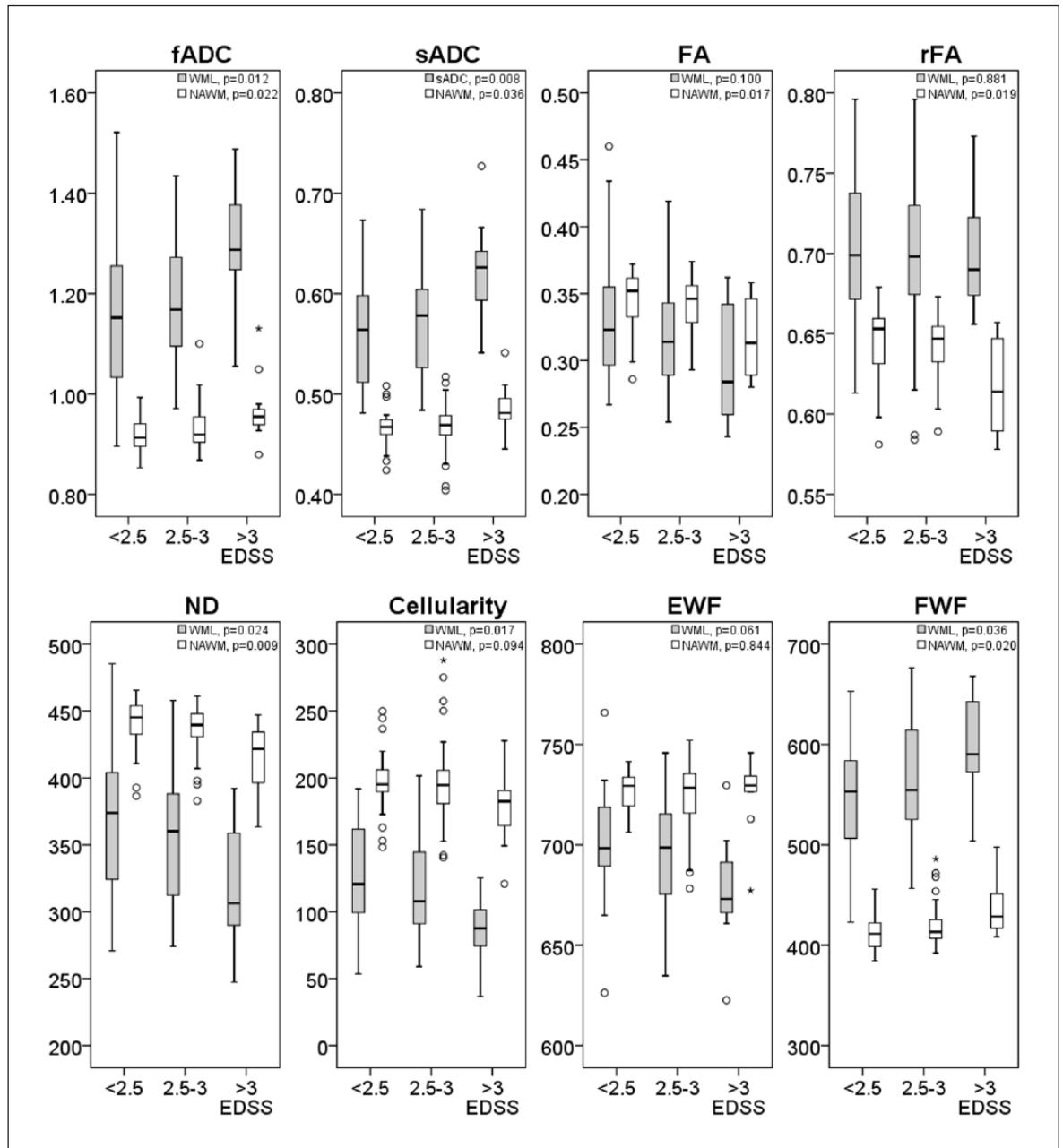


Figure 3. Diffusion parameters in WML and NAWM shown by disability subgroups, $n = 77$. The gray bars represent WML; the white bars represent NAWM. The units are explained in Supplementary material 3. Upper row: fADC, sADC, FA, and rFA in WML (grey bars) and in NAWM (white bars) shown by EDSS subgroups. Lower row: ND, cellularity, EWF, and FWF in WML (grey bars) and in NAWM (white bars) shown by EDSS subgroups. Subgroups are defined by neurological disability: no or minimal (EDSS of <2.5, $n = 27$), low (EDSS of 2.5 or 3.0, $n = 39$), and substantial (EDSS of >3.0, $n = 11$) disability.

EDSS: expanded disability status scale; EWF: extracellular water fraction; fADC: fast apparent diffusion coefficient; FA: fractional anisotropy; FWF: free water fraction; NAWM: normal appearing white matter; ND: neurite density; rFA: restricted fractional anisotropy; sADC: slow apparent diffusion coefficient; WML: white matter lesions.

with disability as measured by EDSS. The sADC was higher in patients with higher disability score. Increased sADC in WML in these patients may be due to greater exchange of intracellular and extracellular

water compartments, possibly caused by demyelination. This is in contrast to the study by Droogan et al.,²⁷ who reported no significant correlation between ADC values in lesions and EDSS. However,

Table 4. Correlations between clinical data, and volumetric and diffusion parameters, $n = 77$.

Volumetric data ^b	EDSS ^a	Disease duration ^a
	r, p	r, p
Whole brain ^c	-0.30, 0.017	-0.11, 0.373
White matter ^c	-0.32, 0.013	-0.05, 0.650
Grey matter ^c	-0.18, 0.129	-0.15, 0.264
Cortex ^c	-0.18, 0.262	-0.06, 0.252
WML volume	0.23, 0.060	0.42, <0.001
% of white matter volume	0.25, 0.048	0.42, <0.001
% of intracranial volume	0.24, 0.055	0.42, <0.001
Diffusion parameters in WML ^d	ρ, p	ρ, p
fADC	0.36, 0.011	0.40, <0.001
sADC	0.31, 0.014	0.29, 0.021
FA	-0.22, 0.073	-0.09, 0.431
rFA	0.01, 0.929	0.13, 0.316
ND	-0.30, 0.015	-0.28, 0.025
Cellularity	-0.27, 0.030	-0.22, 0.094
EWf	-0.34, 0.011	-0.46, <0.001
FWf	0.32, 0.011	0.37, 0.002
Diffusion parameters in NAWM ^d	ρ, p	ρ, p
fADC	0.33, 0.011	0.35, 0.004
sADC	0.23, 0.065	0.15, 0.251
FA	-0.35, 0.011	-0.40, <0.001
rFA	-0.32, 0.011	-0.46, <0.001
ND	-0.39, <0.001	-0.38, 0.002
Cellularity	-0.21, 0.081	-0.13, 0.316
EWf	-0.07, 0.590	-0.08, 0.130
FWf	0.33, 0.011	0.35, 0.004

EDSS: expanded disability status scale; EWf: extracellular water fraction; fADC: fast apparent diffusion coefficient; FA: fractional anisotropy; FWf: free water fraction; NAWM: normal appearing white matter; ND: neurite density; rFA: restricted fractional anisotropy; r : partial correlation; ρ (rho): Spearman's correlation; sADC: slow apparent diffusion coefficient; WML: white matter lesions. Multiple sclerosis severity score (MSSS) did not correlate significantly with any diffusion parameters and is not included in the table.

^aThe p -values are controlled for multiple tests using the Benjamini–Hochberg false discovery rate method; p -values <0.05 are indicated with bold.

^bCorrelations with volumetric data are controlled for age (partial correlation).

^cNormalized to intracranial volume.

^dCorrelations with diffusion parameters are Spearman's correlation (non-normally distributed data).

Gratsias *et al.*¹⁰ reported a correlation between ADC in NAWM and EDSS, in accordance with our results. No correlation between FA in NAWM and EDSS was found in their study. The different results that are reported in these studies may be partly explained by different methodology, since the studies have used different inclusion criteria (different diagnostic criteria over time and differences in study size) as well as different definitions of NAWM (manual defined regions of interest vs segmentation of the whole NAWM). Also the study by Droogan was published back in 1999, using a scanner with lower magnetic field (1.5 T); thus, our study can be of higher imaging quality.

ND in NAWM showed the strongest correlation with EDSS of all tested RSI-derived parameters. This finding indicates that pathological processes may occur in WM outside lesions and may have an impact on the development of disability. Therefore, advanced diffusion techniques like RSI may help explain “the clinico-radiological paradox” understood as a poor association between disability and radiological findings on conventional MRI in MS patients.²⁸ Since ND in theory represents the density of intact axons and dendrites in WM, our results suggest that disability in MS may be associated with diffuse damage of WM rather than with presence of visible lesions on conventional MRI. Our findings support the results recently

published by Brownlee et al.²⁹ reporting an association between neurological disability and low ND values in NAWM obtained in relapse-onset MS patients with the above-mentioned NODDI technique. Interestingly, the significance of correlations between FA, rFA, and ND in NAWM and EDSS still persists after adjustment for disease duration, but disappears after additional adjustment for multiple testing with false discovery rate method. This may be due to the sample size and should be reexamined in a larger study with a broader range of EDSS scores and disease duration.

RSI enables more specific estimation of tissue microstructure and provides more diffusion parameters compared to traditional DWI and DTI.¹⁹ RSI and NODDI have similar approach (multishell acquisition and multicompartiment diffusion model); however, whereas NODDI characterizes the degree of fiber dispersion, RSI further identifies the geometric pattern of dispersion and has a more efficient acquisition time.^{17,30} The association we observe between RSI-derived parameters and disability is very interesting, since an MRI-biomarker for disability in MS is much needed. Clinical disability assessment using EDSS has been criticized, because EDSS mainly reflects motoric disability. Further studies of RSI as a potential biomarker both for physical and cognitive impairment in MS are needed in a larger cohort.

All diffusion parameters investigated in our study differed significantly in pairwise comparisons between WML and NAWM: fADC, sADC, rFA, and FWF measurements were all higher in WML than in NAWM, while values of FA, ND, cellularity, and EWF were lower in WML than in NAWM. Thus, our ADC and FA results are in accordance with previous publications^{10,27} reporting higher ADC and lower FA in WML compared to segmented NAWM regions. Histopathologically, FA correlates with myelin content and axonal count in NAWM and WML.³¹ Lower FA values indicate reduced myelin content and lower number of axons. We found that ND was lower and FWF was higher in WML than in NAWM, which can be explained by reduced number of axons in WML compared to NAWM. This has been reported in previous pathological studies.^{31,32}

Whole brain volume and WM volume normalized to intracranial volume correlated negatively with EDSS (controlled for age) in our study, in line with previous reports: Shiee et al.³³ reported an association between lower WM volume and higher disability in MS patients. WML volume normalized to WM showed a weak positive correlation with disability, and a trend

for weak positive correlation while considering the absolute values. These findings are in general in accordance with other reports where disability in MS patients was reported to weakly correlate with absolute WML volume³⁴ and WML volume normalized to WM.³⁵

A strength of this study is the relatively large study group ($n=77$). Furthermore, the RSI technique used in this study is a promising diffusion MRI method which has not previously been applied in MS, and we used unbiased methods of analysis. One limitation was the lack of a healthy control group. However, our aim was to study this methodology in MS, while others have reported the use of RSI in other conditions. Two experienced MS neurologists at the university hospital examined all the patients, reducing the heterogeneity in both diagnostics and EDSS scores. Another limitation is a large span in lesion volume across the groups (the WML volume in group 1 was 2.7 mL and in group 3 it was 19.7 mL) which could affect the RSI measures in small lesions due to spatial position effect. No longitudinal data were available from these patients for this study, but further studies of this patient cohort are planned.

In conclusion, RSI-derived sADC in WML showed largest difference across disability subgroups and ND in NAWM showed strongest correlation with disability in MS patients. The strongest correlation with EDSS of a parameter obtained in NAWM indicates that pathological processes outside MS-lesions are of importance for disability. Our findings suggest that imaging biomarkers from advanced diffusion techniques like RSI may help explain the “clinico-radiological paradox” and may improve disease monitoring in MS patients. There is a need to study RSI-derived parameters longitudinally in order to evaluate the usefulness of this technique in follow-up of MS patients.

Acknowledgements

The authors would like to thank Anne Hilde Farstad, Martina Jonette Lund, Rigmor Lundby, Wibeke Nordhøy, Niels Petter Sigvartsen, and Tomas Sakinis for assistance.

Declaration of Conflicting Interests

The author(s) declared the following potential conflicts of interest with respect to the research, authorship, and/or publication of this article: P.S. received speaker's fees from Novartis, Genzyme, and Biogen Idec. H.F.H. received an unrestricted research grant from Novartis, and travel support and speaker's fees from Biogen Idec, Genzyme, Novartis, Sanofi-Aventis, and Teva. N.S.W. received a research grant

from General Electric Healthcare (GEHC). E.G.C. received travel support and speaker's fees from Biogen Idec, Genzyme, Merck, Novartis, Sanofi-Aventis, and Teva, and unrestricted research grants from Biogen Idec, Genzyme, and Novartis. Pål Berg-Hansen received an unrestricted research grant from Novartis and travel support and speaker's fees from Novartis, UCB, and Teva. S.M.M. received unrestricted research grant from Novartis and unrestricted travel grant and speaker's fees from Biogen Idec and Novartis. A.B. is a consultant for NordicNeuroLab AS, Bergen, Norway. O.A.A. received speaker's fees from Lundbeck. A.M.D. is a founder of and holds equity in CorTechs Labs, Inc., and serves on its Scientific Advisory Board. He is also a member of the Scientific Advisory Board of Human Longevity, Inc. (HLI) and receives research funding from General Electric Healthcare (GEHC). The terms of these arrangements have been reviewed and approved by the University of California, San Diego in accordance with its conflict of interest policies. M.K.B. received speaker's fees from Novartis and Biogen Idec. H.B. and L.T. W. do not report any conflicts of interest.

Funding

The author(s) disclosed receipt of the following financial support for the research, authorship, and/or publication of this article: This study received funding from South-Eastern Norway Regional Health Authority (project 39569). The project was also supported by grants for MRI acquisitions from the Odd Fellow's Foundation for Multiple Sclerosis Research, Oslo MS Society, Norwegian Society of Radiology and Norwegian Research School in Medical Imaging, and by a travel grant from Ullevålfondet (Ullevål Foundation).

ORCID iD

Anders M Dale  <https://orcid.org/0000-0002-6126-2966>

References

1. Compston A and Coles A. Multiple sclerosis. *Lancet* 2008; 372: 1502–1517.
2. Wattjes MP, Rovira A, Miller D, et al. Evidence-based guidelines: MAGNIMS consensus guidelines on the use of MRI in multiple sclerosis—Establishing disease prognosis and monitoring patients. *Nat Rev Neurol* 2015; 11: 597–606.
3. Thompson AJ, Banwell BL, Barkhof F, et al. Diagnosis of multiple sclerosis: 2017 revisions of the McDonald criteria. *Lancet Neurol* 2017; 17: 162–173.
4. Schaefer PW, Grant PE and Gonzalez RG. Diffusion-weighted MR imaging of the brain. *Radiology* 2000; 217: 331–345.
5. Liu Z and Xiao X. The use of multi b values diffusion-weighted imaging in patients with acute stroke. *Neuroradiology* 2013; 55: 371–376.
6. Alexander AL, Lee JE, Lazar M, et al. Diffusion tensor imaging of the brain. *Neurotherapeutics* 2007; 4: 316–329.
7. Eisele P, Szabo K, Griebel M, et al. Reduced diffusion in a subset of acute MS lesions: A serial multiparametric MRI study. *AJNR Am J Neuroradiol* 2012; 33: 1369–1373.
8. Huang SY, Topyne SM, Nummenmaa A, et al. Characterization of axonal disease in patients with multiple sclerosis using high-gradient-diffusion MR imaging. *Radiology* 2016; 280: 244–251.
9. Inal M, Unal B, Kala I, et al. ADC evaluation of the corticospinal tract in multiple sclerosis. *Acta Neurol Belg* 2015; 115: 105–109.
10. Gratsias G, Kapsalaki E, Kogia S, et al. A quantitative evaluation of damage in normal appearing white matter in patients with multiple sclerosis using diffusion tensor MR imaging at 3 T. *Acta Neurol Belg* 2015; 115: 111–116.
11. Temel S, Keklikoglu HD, Vural G, et al. Diffusion tensor magnetic resonance imaging in patients with multiple sclerosis and its relationship with disability. *Neuroradiol J* 2013; 26: 3–17.
12. Genova HM, DeLuca J, Chiaravalloti N, et al. The relationship between executive functioning, processing speed, and white matter integrity in multiple sclerosis. *J Clin Exp Neuropsychol* 2013; 35: 631–641.
13. Kurtzke JF. Rating neurologic impairment in multiple sclerosis: An expanded disability status scale (EDSS). *Neurology* 1983; 33: 1444–1452.
14. Phuttharak W, Galassi W, Laopaiboon V, et al. ADC measurements in various patterns of multiple sclerosis lesions. *J Med Assoc Thai* 2006; 89: 196–204.
15. Anik Y, Demirci A, Efendi H, et al. Evaluation of normal appearing white matter in multiple sclerosis: Comparison of diffusion magnetic resonance, magnetization transfer imaging and multivoxel magnetic resonance spectroscopy findings with expanded disability status scale. *Clin Neuroradiol* 2011; 21: 207–215.
16. Beaulieu C. The basis of anisotropic water diffusion in the nervous system—A technical review. *NMR Biomed* 2002; 15: 435–455.
17. Zhang H, Schneider T, Wheeler-Kingshott CA, et al. NODDI: Practical in vivo neurite orientation

- dispersion and density imaging of the human brain. *Neuroimage* 2012; 61: 1000–1016.
18. White NS, Leergaard TB, D’Arceuil H, et al. Probing tissue microstructure with restriction spectrum imaging: Histological and theoretical validation. *Hum Brain Mapp* 2013; 34: 327–346.
19. White NS, McDonald C, Farid N, et al. Diffusion-weighted imaging in cancer: Physical foundations and applications of restriction spectrum imaging. *Cancer Res* 2014; 74: 4638–4652.
20. White NS, McDonald CR, Farid N, et al. Improved conspicuity and delineation of high-grade primary and metastatic brain tumors using “restriction spectrum imaging”: Quantitative comparison with high B-value DWI and ADC. *AJNR Am J Neuroradiol* 2013; 34: 958–64.
21. McDonald CR, White NS, Farid N, et al. Recovery of white matter tracts in regions of peritumoral FLAIR hyperintensity with use of restriction spectrum imaging. *AJNR Am J Neuroradiol* 2013; 34: 1157–1163.
22. Loi RQ, Leyden KM, Balachandra A, et al. Restriction spectrum imaging reveals decreased neurite density in patients with temporal lobe epilepsy. *Epilepsia* 2016; 57: 1897–1906.
23. Polman CH, Reingold SC, Banwell B, et al. Diagnostic criteria for multiple sclerosis: 2010 revisions to the McDonald criteria. *Ann Neurol* 2011; 69: 292–302.
24. Roxburgh RH, Seaman SR, Masterman T, et al. Multiple Sclerosis Severity Score: Using disability and disease duration to rate disease severity. *Neurology* 2005; 64: 1144–1151.
25. Verma RK, Slotboom J, Locher C, et al. Characterization of enhancing MS lesions by dynamic texture parameter analysis of dynamic susceptibility perfusion imaging. *Biomed Res Int* 2016; 2016: 9578139.
26. Toh CH, Wei KC, Ng SH, et al. Differentiation of tumefactive demyelinating lesions from high-grade gliomas with the use of diffusion tensor imaging. *AJNR Am J Neuroradiol* 2012; 33: 846–851.
27. Droogan AG, Clark CA, Werring DJ, et al. Comparison of multiple sclerosis clinical subgroups using navigated spin echo diffusion-weighted imaging. *Magn Reson Imaging* 1999; 17: 653–661.
28. Barkhof F. The clinico-radiological paradox in multiple sclerosis revisited. *Curr Opin Neurol* 2002; 15: 239–245.
29. Brownlee W, Alves Da Mota P, Prados F, et al. Neurite Orientation Dispersion and Density Imaging (NODDI) is sensitive to microstructural damage related to disability in relapse-onset MS. *Neurology* 2016; 16 Supplement/S41.003.
30. Reas ET, Hagler DJ, White NS, et al. Sensitivity of restriction spectrum imaging to memory and neuropathology in Alzheimer’s disease. *Alzheimers Res Ther* 2017; 9: 55.
31. Schmierer K, Wheeler-Kingshott CA, Boulby PA, et al. Diffusion tensor imaging of post mortem multiple sclerosis brain. *Neuroimage* 2007; 35: 467–477.
32. Stadelmann C, Wegner C and Bruck W. Inflammation, demyelination, and degeneration - recent insights from MS pathology. *Biochim Biophys Acta* 2011; 1812: 275–282.
33. Shiee N, Bazin PL, Zackowski KM, et al. Revisiting brain atrophy and its relationship to disability in multiple sclerosis. *PLoS ONE* 2012; 7: e37049.
34. Mammi S, Filippi M, Martinelli V, et al. Correlation between brain MRI lesion volume and disability in patients with multiple sclerosis. *Acta Neurol Scand* 1996; 94: 93–96.
35. Nygaard GO, Walhovd KB, Sowa P, et al. Cortical thickness and surface area relate to specific symptoms in early relapsing-remitting multiple sclerosis. *Mult Scler* 2015; 21: 402–414.